

## Transport of silica encapsulated DNA microparticles in controlled instantaneous injection open channel experiments

Tang, Yuchen; Foppen, Jan Willem; Bogaard, Thom A.

**DOI**

[10.1016/j.jconhyd.2021.103880](https://doi.org/10.1016/j.jconhyd.2021.103880)

**Publication date**

2021

**Document Version**

Final published version

**Published in**

Journal of Contaminant Hydrology

**Citation (APA)**

Tang, Y., Foppen, J. W., & Bogaard, T. A. (2021). Transport of silica encapsulated DNA microparticles in controlled instantaneous injection open channel experiments. *Journal of Contaminant Hydrology*, 242, Article 103880. <https://doi.org/10.1016/j.jconhyd.2021.103880>

**Important note**

To cite this publication, please use the final published version (if applicable). Please check the document version above.

**Copyright**

Other than for strictly personal use, it is not permitted to download, forward or distribute the text or part of it, without the consent of the author(s) and/or copyright holder(s), unless the work is under an open content license such as Creative Commons.

**Takedown policy**

Please contact us and provide details if you believe this document breaches copyrights. We will remove access to the work immediately and investigate your claim.



# Transport of silica encapsulated DNA microparticles in controlled instantaneous injection open channel experiments

Yuchen Tang<sup>a,\*</sup>, Jan Willem Foppen<sup>a,b</sup>, Thom A. Bogaard<sup>a</sup>

<sup>a</sup> Water Resource Section, Department of Civil Engineering and Geoscience, Delft University of Technology, Delft, Netherlands

<sup>b</sup> IHE Delft Institute for Water Education, Delft, Netherlands

## ARTICLE INFO

### Keywords:

Microparticle tracers  
DNA  
Surface water  
Hydrodynamic dispersion

## ABSTRACT

Surface water tracing is a widely used technique to investigate in-stream mass transport including contaminant migration. Recently, a microparticle tracer was developed with unique synthetic DNA encapsulated in an environmentally-friendly silica coating (Si-DNA microparticle). Previous tracing applications of such tracers reported detection and quantification, but a massive loss of tracer mass. However, the transport behavior of these DNA-tagged microparticle tracers has not been rigorously quantified and compared with that of solute tracers. Therefore, we compared the transport behavior of Si-DNA microparticles to the behavior of solute NaCl in 6 different, environmentally representative water types using breakthrough curves (BTCs), obtained from laboratory open channel injection experiments, whereby no Si-DNA microparticle tracer mass was lost. Hereafter, we modelled the BTCs using a 1-D advection-dispersion model with one transient storage zone (OTIS) by calibrating the hydrodynamic dispersion coefficient  $D$  and a storage zone exchange rate coefficient. We concluded that the transport behavior of Si-DNA microparticles resembled that of NaCl in surface-water relevant conditions, evidenced by BTCs with a similar range of  $D$ ; however, the Si-DNA microparticle had a more erratic BTC than its solute counterpart, whereby the scatter increased as a function of water quality complexity. The overall larger confidence interval of  $D_{\text{Si-DNA}}$  was attributed to the discrete nature of colloidal particles with a certain particle size distribution and possibly minor shear-induced aggregations. This research established a solid methodological foundation for field application of Si-DNA microparticles in surface water tracing, providing insight in transport behavior of equivalent sized and mass particles in rivers.

## 1. Introduction

Environmental pollution poses an unprecedented burden over surface water quality and aquatic ecosystems. Between terrestrial and marine ecosystems, rivers are the major dispersal vectors both to distribute nutrient and to transport detrimental contaminants (Nantke et al., 2019). A comprehensive understanding of riverine mass transport is a prerequisite for pollution control. Solute and particle tracers are widely used in surface water tracing experiments to characterize in-stream transport of solutes and particulates. Most of such studies use solute tracers, such as to track sources and migration pathways of pollutants, sediment-water interactions, and transient storages (Bencala et al., 2011; Haggerty et al., 2008). Particle tracers, however, were used only in a few studies, e.g., micron-sized fluorescent microspheres, bacteriophages/bacteria, and natural clay/sediment particles (Göppert and Goldscheider, 2008; Jamieson et al., 2005; Schipperski et al., 2016;

Spencer et al., 2011; Wyer et al., 2010). In these studies and as far as we know, particles smaller than  $\leq 1 \mu\text{m}$  were only used once due to practical limitations (Goepfert and Goldscheider, 2019). However, colloids, defined as materials between 10 nm and 10  $\mu\text{m}$  (McCarthy and Zachara, 1989), in the aquatic environment are of significant interest due to their sizes, surface areas, and mass: as nutrients in phosphorus related colloids (Guo and Macdonald, 2006; Heathwaite and Dils, 2000; Jarvie et al., 2012; Stolpe et al., 2010), as carriers for contaminants (Lead and Wilkinson, 2006; H. Wang et al., 2015), and, when smaller than  $\sim 30 \text{ nm}$ , their -limited- sizes may cause enhanced biological and chemical reactivities (Auffan et al., 2009; Azimzade et al., 2021). These aquatic colloids include naturally occurring biocolloids (e.g., viruses, bacteria, extracellular polymeric substances, etc.), geocolloids (e.g., clay, metal oxides and hydroxides), anthropogenic engineered nanomaterials (e.g., titanium dioxide nanoparticles and carbon nanotubes) and microplastics (Alimi et al., 2018; H. Wang et al., 2015; Xu et al., 2020; Zhu et al.,

\* Corresponding author.

E-mail addresses: [Y.Tang-3@tudelft.nl](mailto:Y.Tang-3@tudelft.nl) (Y. Tang), [j.foppen@un-ihe.org](mailto:j.foppen@un-ihe.org) (J.W. Foppen), [t.a.bogaard@tudelft.nl](mailto:t.a.bogaard@tudelft.nl) (T.A. Bogaard).

<https://doi.org/10.1016/j.jconhyd.2021.103880>

Received 15 September 2020; Received in revised form 31 July 2021; Accepted 16 August 2021

Available online 23 August 2021

0169-7722/© 2021 The Authors. Published by Elsevier B.V. This is an open access article under the CC BY license (<http://creativecommons.org/licenses/by/4.0/>).

2021). Besides, traditional tracer tests have several disadvantages: 1) a limited number of distinguishable artificial tracers is available, 2) tracer detections often have background noise with dilution limitations, and 3) practical constraints limit the application of a proper tracer (e.g., strict regulations for uranine or rhodamine or being very expensive like fluorobenzoic acid) (Bencala et al., 2011; Choi et al., 2000; Stern et al., 2001; Whitmer et al., 2000; Wilderer, 2011).

In search of new tracer substances, synthetic DNA (deoxyribonucleic acid) was introduced as a hydrological tracer. Laboratory synthesis enables a virtually unlimited number of synthetic DNA sequences to be produced, and these can be identified by target specific quantitative Polymerase Chain Reaction (qPCR), with a theoretical detection limit down to one DNA molecule per qPCR well (Watson et al., 1992). Such DNA tracers have been employed to identify pathways of sediments and solutes in various environmental conditions (Aquilanti et al., 2013, 2016; Dahlke et al., 2015; Foppen et al., 2011, 2013; Mahler et al., 1998; McCluskey et al., 2021; Pang et al., 2017; Ptak et al., 2004; Sabir et al., 1999, 2000; Viccione et al., 2014). However, these 'naked' DNA tracers showed attenuation up to 80–90% of injected mass, which was mainly attributed to adsorption, attachment and biological uptake (Dahlke et al., 2015; Foppen et al., 2013). Besides, DNA strands are subject to breakdown and degradation in the natural environment due to extracellular enzymes, abundant microbial activity, or elevated temperatures (Lindahl, 1993; Sabir et al., 1999; Tsuji et al., 2017).

Such DNA mass loss may be overcome by using a 'cover' to protect the DNA strands from the hostile environment. So far, silica-coated DNA-encapsulated microparticles (Si-DNA microparticles) and similar variants have been applied in hydrological tracing experiments as proof of concept (Garnett et al., 2009; Liao et al., 2020; Pang et al., 2014; Paunescu et al., 2013; Puddu et al., 2014; A. Sharma et al., 2021; A. N. Sharma et al., 2012). In multiplexed tracing experiments in streams and rivers, DNA-tagged microparticles were traceable at greater distances compared to solute tracers and exhibited similar breakthrough behavior (Garnett et al., 2009; Pang et al., 2020; A. N. Sharma et al., 2012). However, the transport behavior of these DNA-tagged microparticle tracers has not been rigorously quantified and compared with that of solute tracers. A mass balance accounting for sources and sinks is required for the understanding of Si-DNA microparticles in transport behavior. Furthermore, between DNA-tagged microparticles and ubiquitous natural substances in the aquatic environment (i.e., organic and inorganic particles), possible interactions should also be considered when necessary. Such knowledge is essential when selecting appropriate tracers for hydrological investigations.

Therefore, the objective of this paper was to understand and quantify the transport behavior of Si-DNA microparticles in surface water tracing experiments. Our hypothesis was that, when in colloidal stable conditions, Si-DNA microparticles have a transport behavior comparable to solute tracers in surface water injection experiments. Hereto, we conducted a series of controlled injection experiments in 6 environmentally representative water types and compared the breakthrough curves (BTCs) and hydrodynamic dispersion coefficient  $D_{\text{Si-DNA}}$  of Si-DNA microparticles to that of NaCl, a solute tracer ( $D_{\text{NaCl}}$ ). Besides, these laboratory-scale experiments are vital for successful field-scale tracing experiments, for which a well-developed methodology including reliable sample-handling technique is indispensable (Mikutis et al., 2018). This paper contributes to understanding the behavior of such novel DNA-tagged microparticle and anticipates the application potential in large-scale tracing experiments, providing insight in transport behavior of equivalent sized and mass particles in rivers.

## 2. Material & methods

### 2.1. Si-DNA microparticles and primers

The Si-DNA microparticles were the same as used in the study by Mikutis et al., 2018 (provided by ETH Zurich). The synthesized Si-DNA

microparticles were spheres with a narrow and unimodal size distribution. The surface of Si-DNA microparticles represents  $\text{SiO}_2$  properties and no interference with DNA chemistry is expected (Paunescu et al., 2013). DNA and primer sequences are given in the Supporting Information (Table S1 in the SI).

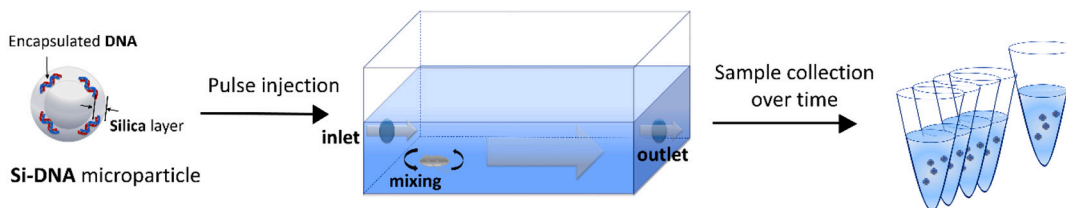
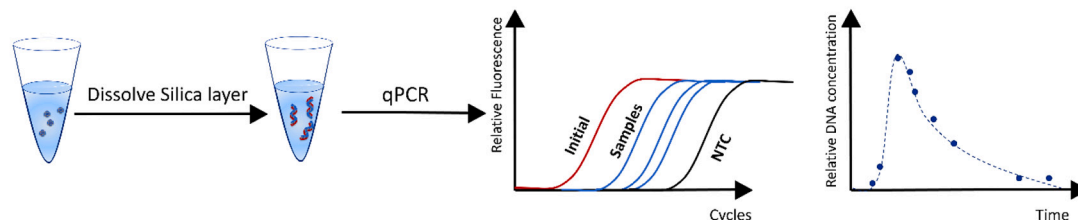
### 2.2. Hydrodynamic radius and zeta potential of Si-DNA microparticles

The hydrodynamic radius ( $R_{\text{hDLS}}$ ) of Si-DNA microparticles in each water type (~500 ppb) was measured by Dynamic Light Scattering (DLS), and the zeta potential ( $\zeta$ ) of Si-DNA microparticles was calculated by using Smoluchowski's equation from their electrophoretic mobility measured on a NanoSizer (Nano Series, Malvern Instrument Ltd., Worcestershire, United Kingdom). To assess if aggregations of Si-DNA microparticles took place within the time frame of the injection experiment, in each water type the  $R_{\text{hDLS}}$  was measured as a function of time in quiescent and in mixing conditions, respectively. Thereto, in each water type, Si-DNA microparticles were suspended to reach a final concentration of ~500 ppb of 2 mL in duplicate. Each sample tube was sonicated to reach a homogenous suspension before the first measurement. After the first measurement of  $R_{\text{hDLS}}$ , one sample was allowed to stand still while the other sample was mixed at 1500 rpm until the next measurement in 2 h.

### 2.3. Injection experiments

Injection experiments of tracers are widely conducted to obtain BTCs to understand transport behavior because they are simple to carry out and give good and reliable results (Leibundgut and Seibert, 2011). A series of pulse-injection experiments with Si-DNA microparticles was performed in 6 water types in a horizontally-placed PVC box (Fig. 1). The channel was 20 cm long, 10 cm wide, and 3 cm deep. Tracers were injected by a peristaltic pump. The injection experiment had a flow rate of ~18 mL/min and a duration of approximately 100 min (hydraulic retention time was ~28.5 min). For each experiment, a 10 mL suspension of ~5 ppb Si-DNA microparticles was injected. Due to the low flow rate, a magnetic stirrer was set close (~2 cm) to the inlet point to enhance cross-sectional mixing of tracer mass. We assumed that tracer mass was mixed rapidly, but not instantaneous, over the entire cross-section, so that the impact of the mixing in the so-called initial period on the transport in the investigated reach was negligible (Rieckermann et al., 2005), whereby the mixing was not represented by the 1-D advection-dispersion process. A solute fluorescent dye tracer was added once to visualize mixing conditions and the transport pathway of the injected tracer mass in the box (see details in the SI). Sampling was carried out at the outlet. The sampling interval progressively increased from 1 to 5 min (see Table S2 in the SI). From each of the sample bottle, 500  $\mu\text{L}$  of sub-sample was taken (in duplicate) for sample analysis. Sample bottles were vortexed for 1 to 2 min before taking sub-samples, ensuring that Si-DNA microparticles were homogeneously distributed over the entire sample volume. Each injection experiment was performed three times. The 1st and 2nd injection experiments were sequentially performed with a break of 0.5 h to rinse the set-up to remove possible residual substances from the previous experiment. The 3rd injection experiment was performed later. After each experiment, extra water samples were analyzed for any residual tracer in the PVC box (see Fig. 1).

First, a pulse-injection experiment of NaCl (5.0 mM, EMSURE®, Merck KGaA), a solute tracer, was performed in triplicate for reference. The BTC of NaCl was measured by an electrical conductivity (EC) meter (Multi 3620 IDS, Xylem Analytics Germany GmbH, Germany), and mass recovery was calculated (see the standard curve on Page S5 in the SI). Similarly to the NaCl injection experiment, Si-DNA microparticle tests were conducted in 6 representative water types. Demi water was chosen as a 'blank' control. Furthermore, we used a 5.0 mM  $\text{NaH}_2\text{PO}_4 \cdot \text{H}_2\text{O}$  solution (J.T. Baker), and a 1.67 mM  $\text{CaCl}_2 \cdot 2\text{H}_2\text{O}$  (EMSURE®, Merck

**(1) Injection experiment****(2) pre- and post-qPCR procedure**

**Fig. 1.** Schematic of injection experiment and sample analysis procedure (figure inspired by Mikutis et al., 2018). (1) Injection experiment plot: after a pulse injection of Si-DNA microparticles into the PVC box (20 cm × 10 cm × 3 cm), the particles were transported along with the water flow from left to right. (2) pre and post qPCR procedure: the silica layer is dissolved before qPCR analysis. The qPCR readings are converted into DNA concentration and plotted as a function of time resulting in a BTC.

KGaA) solution to anticipate the effects of monovalent (Dalas and Koutsoukos, 1990; Ji et al., 2020) and divalent cations (Liu et al., 2010). This group of synthetic chemical solutions were prepared in the laboratory. Tap water was used as a transition water type, which was more complex than the synthetic chemical solutions, but less complex than natural water in the sense that various natural or anthropogenic nanoparticles, colloidal particles or particulate matter (>5 μm) could still be part of that water. Also, two natural surface water samples were collected from a canal in Delft, one of which was filtered (5-μm cellulose nitrate filters; referred to as “Filtered natural water”), and the other was not (referred to as “Natural water”). The canal receives its water from both Rhine River and Meuse River. In this way, we tested for the effect of particulate matter. Concentrations of major cations and anions of Tap water and Natural water samples were measured by ion chromatography (Methrohm AG). When performing the 3rd series of replicate experiments, the organic matter content of the water types was measured as dissolved organic carbon (DOC, in mg-C/L) using the combustion technique with a total organic carbon analyser (TOC-VCNP (TN), Shimadzu, Japan).

Before the injection experiments, to assess if the PVC material could be a possible sink for DNA mass loss during injection experiments, the concentration of Si-DNA microparticles in Demi water was determined as a function of time in batch experiments for 7 days (an extended period was designed as an extreme condition). The suspension of Si-DNA microparticles in Demi water was kept in PVC containers and protected against daylight at room temperature. No mass loss of Si-DNA microparticles was observed (results shown in Fig. S3 in the SI).

#### 2.4. Sample analysis

Quantitative Polymerase Chain Reaction (qPCR) was used to quantify DNA concentrations of the samples from the injection experiments. Prior to qPCR analysis, samples were centrifuged, washed and re-suspended before dissolving silica-coating. After extensive testing, some adjustments were made to the original protocol in Paunescu et al. (2013), such as increasing centrifugal force and duration, washing samples with Demi water, and enhanced mixing (see Centrifugation

procedure and quality control in the SI.). To minimize manual errors, a high-precision pipetting robot (QIAgility benchtop instrument) was used to mix reagents. The silica-coating was dissolved within 10 min by adding 1 μL Buffered Oxide Etch (BOE) solution (2.3 g of NH<sub>4</sub>FHF (Sigma Aldrich) and 1.9 g of NH<sub>4</sub>F (J.T.Baker) in 10 mL water to achieve a final concentration of 2500 ppm F<sup>-</sup> ions). After the silica-coating had dissolved, the sample was directly used for qPCR reaction without purification. qPCR was performed using KAPA SYBR Green based master mixes (Roche Sequencing and Life Science) on a Bio-Rad MiniOpticon. The details of qPCR reaction setup and cycling parameters are provided in the SI. The qPCR readings (i.e., C<sub>q</sub>) were converted into DNA concentration (mg/mL) and plotted against time to produce a BTC (Fig. 1). The conversion equation and mass recovery calculations are provided in the SI. Hereafter, we compared the obtained BTCs of Si-DNA microparticles with that of NaCl.

#### 2.5. Analysis of BTCs

The physical transport of solutes and Si-DNA microparticles in the injection experiments can be described by a one-dimensional advection and dispersion equation with a first-order mass transfer transient storage. We used the One-dimensional Transport with Inflow and Storage model (OTIS) to model the curves (Runkel, 1998). OTIS was chosen because our experimental set-up mimics 1-D steady uniform flow in a main channel with a storage-zone without lateral inflow. Besides, DNA mass was conserved during injection experiments, since no source or sink of DNA mass was observed in our experimental channel. Therefore, no mass-loss term was considered in the OTIS modelling. The goals were to fit the observed BTC and to quantify  $D_{Si-DNA}$  of the Si-DNA microparticles. The fitting was carried out using Nonlinear Least Squares by requiring an input of observed BTC (see details in the SI), which was implemented in OTIS-P. In a modelling case where mass is conserved, the injected mass should equal to the recovered total mass, which is the area under the observed BTC. In spite of no mass loss, this total recovered DNA mass calculated from the observed BTC can differ from the measured injected DNA mass to some extent (see more discussion in 3.2). To resolve the imbalance of input/output mass, we scaled the mass

recoveries to 100% by linearly correcting the initial injection mass before OTIS modelling. This linear correction of the injected mass has no influence on the characteristics of the BTCs (Pang et al., 2017) and can be used for dispersion estimation in OTIS-p.

$$\frac{\partial C}{\partial t} = -\frac{Q}{A} \frac{\partial C}{\partial x} + \frac{1}{A} \frac{\partial}{\partial x} \left( AD \frac{\partial C}{\partial x} \right) + \alpha(C_S - C) \quad (1)$$

$$\frac{dC_S}{dt} = \alpha \frac{A}{A_S} (C - C_S) \quad (2)$$

Where  $A$  is the main channel cross-sectional area [ $\text{m}^2$ ],  $A_S$  the storage zone cross-sectional area [ $\text{m}^2$ ],  $C$  the main channel solute concentration [ $\text{g}/\text{m}^3$ ],  $C_S$  the storage zone solute concentration [ $\text{g}/\text{m}^3$ ],  $D$  the dispersion coefficient [ $\text{m}^2/\text{s}$ ],  $Q$  the volumetric flow rate [ $\text{m}^3/\text{s}$ ],  $t$  time [ $\text{s}$ ],  $x$  distance [ $\text{m}$ ], and  $\alpha$  the storage zone exchange coefficient [ $1/\text{s}$ ].

In OTIS-P,  $D$  and  $\alpha$  were fitted while other parameters were fixed. Best-fit estimates of  $D_{\text{NaCl}}$  and  $\alpha_{\text{NaCl}}$  from NaCl injection experiments were used as initial estimates of  $D_{\text{Si-DNA}}$  and  $\alpha_{\text{Si-DNA}}$ .

### 3. Results & discussion

#### 3.1. BTCs of Si-DNA microparticles and the effect of water quality & hydrodynamics

Water quality (pH, EC, DOC, TSS and major chemical compositions) of 6 water types used for the injection experiments are given in Table 1. The zeta potential of the Si-DNA microparticles was between  $-17 \pm 7.1$  mV and  $-49.8 \pm 5.9$  mV, and the mean  $R_{\text{hdLS}}$  was between  $\sim 237 \pm 81$  nm and  $\sim 299 \pm 129$  nm (measured before the injection experiments, Table 1). In the quiescent condition and as a function of time, the mean  $R_{\text{hdLS}}$  and PDI of Si-DNA microparticles remained constant for each water type (Fig. 2 a). A one-way ANOVA revealed that there was no significant difference ( $p = 0.3$ , at 95% significance level) among mean  $R_{\text{hdLS}}$  and PDI of Si-DNA microparticles. However, when mixing, the  $R_{\text{hdLS}}$  and PDI significantly increased ( $p$  values  $< 0.05$ , at 95% significance level) in  $\text{CaCl}_2$ , Tap water, filtered and unfiltered Natural water, while in Demi water and in Phosphate solution the  $R_{\text{hdLS}}$  and PDI remained constant as a function of time (Fig. 2 b).

Generally, the BTCs of the Si-DNA microparticles in all water types showed a close resemblance to the BTCs of NaCl (Fig. 3, S7). The  $C/C_0$  (%) of the NaCl BTC demonstrated a sharp increase and then reached a peak of roughly 2% (at  $\sim 4$ th minute), which was followed by a slow decline ( $\sim 1\%$  at  $\sim 24$  min; Fig. 3). When compared with Si-DNA microparticles, the  $C/C_0$  of Si-DNA microparticles were 'noisier' than the NaCl BTC. Moreover, comparing Si-DNA BTCs within the group of laboratory prepared waters, the BTCs in  $\text{CaCl}_2$  were slightly 'noisier' than those in Demi and  $\text{NaH}_2\text{PO}_4$ . Also, the Si-DNA BTCs were more scattered in Tap water, Filtered natural water, and Natural water. In other words, the observed relative concentrations of Si-DNA microparticles around the peaks were more scattered as compositions of solution became more complex, exhibiting higher peak values than those of NaCl tracers. In particular, the Si-DNA BTCs in the Filtered natural water and Natural water were most scattered with the largest discrepancy among the triplicates.

Water quality including ionic strength, natural organic matter (NOM) content, and suspended solids are important factors determining the fate of engineered nano- and micro-particles in water bodies (Shevlin et al., 2018). In our experiments, the ionic strength of used water types was in the range of 1–25 mM, based on the measured concentrations of known cations and anions (Table 1). Note that compared to studies which focused on the effect of ionic strength on colloidal interactions (Ledín and Karlsson, 1993; J. F. McCarthy et al., 2002; Nocito-Gobel and Tobiasson, 1996; Torkzaban et al., 2008; Zhao et al., 2021), the ionic strength of water types used in this paper was in the low range. In such solution chemistry, Si-DNA microparticles remained colloidally stable,

evidenced by a constant hydrodynamic radius over 4 h (Fig. 2. a). This indicated that the solution chemistry alone was unfavorable for aggregation of Si-DNA microparticles (Metin et al., 2014). Specifically, the calculated total energy barriers based on Classical DLVO theory (Derjaguin and Landau, 1993; Verwey, 1947) for Si-DNA microparticles in Demi and  $\text{NaH}_2\text{PO}_4$  solution were relatively high ( $\geq 50$  kT, with negligible secondary minima, see table S3 in the SI for the details of DLVO energy calculations). Such high repulsive energy would prevent aggregation of Si-DNA microparticles in the solution chemistry.

In  $\text{CaCl}_2$ , Tap, Filtered natural and Natural waters, the reduction of zeta potentials (Table 1) can be explained by the compression of the electric double layer, indicating a likely lower total energy barrier (Elimelech et al., 2013). In contrast to the quiescent condition (no shear force), after 2 h of mixing, the increase of  $R_{\text{hdLS}}$  in  $\text{CaCl}_2$ , Phosphate, Tap, filtered and unfiltered natural water (Fig. 2 b) indicated shear-induced aggregation (i.e., orthokinetic flocculation) (Barthelmes et al., 2003; Hijnen and Clegg, 2014; Spicer, 1997). Moreover, when a flow field acts on the suspension, the hydrodynamic force (e.g. shear force) is responsible for bringing the particles together and would likely dominate the particle collisions (Elimelech et al., 2013; Frungieri et al., 2020; Zaccone et al., 2009). Thus, it is reasonable to imply that shear-induced aggregation might have taken place during the injection experiments. However, we argue that the effect of aggregation is likely minor, as the coupled effect of shear rate and volume friction (Gregory, 2005) in our experiments was orders of magnitude lower than that in our batch mixing experiments.

The BTCs of Si-DNA microparticles in filtered and unfiltered natural water showed similar characteristics with a degree of scatter in the peaks (Fig. 3), despite the variations in water quality parameters between the third and the preceding two series of experiments (Table 1, there was a time gap between the first two series and the third series). The interactions between natural particulates and nanoparticles were extensively studied in literature (Lead et al., 2018; Oney and Nason, 2021; Peijnenburg et al., 2015; Petosa et al., 2010; Praetorius et al., 2020; Quik et al., 2013; Velzeboer et al., 2014; Xu et al., 2020). For example, Quik and co-workers found that natural particulates played a key role in the increased hetero-aggregation and sedimentation of nanomaterials by comparing filtered and unfiltered natural water samples (Quik et al., 2013). However, the effect of particulate matter content ( $\geq 5 \mu\text{m}$ ) on the transport characteristics of Si-DNA microparticle was not clearly observed in our injection experiments.

#### 3.2. $D$ and colloidal stability

After re-scaling mass recoveries to 100% without changing the BTC behavior, we modelled the BTCs of all injection experiments to determine  $D$  and  $\alpha$  (Fig. 4 and Table 1). The rising and falling limbs of NaCl BTCs were modelled almost perfectly (Fig. 3 panel a,  $R^2 = 99.8\%$ ), and the peaks of NaCl BTCs were slightly underestimated. This showed that the OTIS conceptualization (1D ADE with one transient storage) was well capable of mimicking the experimental set-up even though there was a small discrepancy between the schematisation of OTIS and experimental set-up. In the 1D representation in OTIS the tracer mass is uniformly distributed over the cross-sectional area. We used a stirrer to achieve cross-sectional mixing, and the time required to achieve this was not incorporated in our OTIS modelling. Meanwhile, stirring enhanced the extent of the interaction between tracers and the storage zone, so that tracer spreading caused by storage exchange reached an equilibrium stage soon after tracers entered the channel (Harvey and Wagner, 2000). This storage contribution was visible in the long tail of the BTCs, indicating a diffusion limited steady-state storage. Moreover, the calculated Damkohler number ( $\text{DaI}$  is  $\sim 10$ , see Eq. (S6) in the SI) also suggested the dominance of the storage process, caused by enhanced mixing. Thus, fitting the resultant long tail using a higher exchange rate compromised the fitting of the peak (details of OTIS model implementation are provided in the SI). This effect could also be seen in the

**Table 1**  
Water quality,  $\zeta$ ,  $R_{hDLS}$ , mass recoveries, and  $D$  &  $\alpha$  of Si-DNA microparticles in 6 water types for injection experiments in triplicate.

Water types	pH	EC [ $\mu$ S/cm]	DOC [mg-C/L]	TSS [mg/L]	Na <sup>+</sup>	K <sup>+</sup>	Ca <sup>2+</sup>	Mg <sup>2+</sup>	Cl <sup>-</sup>	NO <sub>3</sub> <sup>-</sup>	PO <sub>4</sub> <sup>3-</sup>	SO <sub>4</sub> <sup>2-</sup>	$\zeta$ [mV]	$R_{hDLS}$ <sup>1</sup> [nm]	M.R. [%]	$\alpha$		$D \times 10^{-3}$	
																[1/s]	95% C.L. [ $\pm$ ]	[m <sup>2</sup> /s]	95% C.L. [ $\pm$ ]
Demi water	6.4 $\pm$ 0.25	0.5 $\pm$ 0.01	0.73 $\pm$ 0.01	-	-	-	-	-	-	-	-	-	-38 $\pm$ 5.3	242 $\pm$ 81	91	1.99	1.12	3.96	1.17
													-30 $\pm$ 6.2	243 $\pm$ 79	97	1.03	0.18	2.81	0.51
													-21 $\pm$ 4.5	288 $\pm$ 103	102	1.60	0.81	3.91	1.26
CaCl <sub>2</sub>	5.8 $\pm$ 0.01	427 $\pm$ 7	0.51 $\pm$ 0.01	-	-	-	68 $\pm$ 1.5	-	117 $\pm$ 0.5	-	-	-	-22 $\pm$ 5.4	259 $\pm$ 93	N.	1.29	0.39	2.81	0.76
													-21 $\pm$ 4.5	288 $\pm$ 103	111	1.97	1.20	4.54	1.38
													-22 $\pm$ 5.4	259 $\pm$ 93	N.	1.29	0.39	2.81	0.76
Pho	7.2 $\pm$ 0.05	787 $\pm$ 5	0.57 $\pm$ 0.01	-	170 $\pm$ 3	-	-	-	14 $\pm$ 0.5	-	478 $\pm$ 5	-	-50 $\pm$ 5.9	259 $\pm$ 111	80	1.66	1.19	4.44	1.88
													-49 $\pm$ 5.6	284 $\pm$ 128	84	1.63	0.53	3.48	0.75
													-49 $\pm$ 5.6	284 $\pm$ 128	98	1.22	0.16	3.10	0.37
Tap water	8.1 $\pm$ 0.1	522 $\pm$ 5	-	-	40 $\pm$ 0.5	46 $\pm$ 1	49 $\pm$ 2.5	7 $\pm$ 0.5	61 $\pm$ 8	9 $\pm$ 0.1	-	47 $\pm$ 5	-24 $\pm$ 4.5	237 $\pm$ 81	94	3.44	1.41	4.91	0.69
													-18 $\pm$ 5.4	261 $\pm$ 108	N.	1.36	0.72	3.26	1.32
													-18 $\pm$ 5.4	261 $\pm$ 108	N.	1.36	0.72	3.26	1.32
Filtered natural water <sup>2</sup>	8.0 $\pm$ 0.2	780 $\pm$ 3	-	-	60 $\pm$ 2	73 $\pm$ 1	73 $\pm$ 2	15 $\pm$ 1	94 $\pm$ 2	2 $\pm$ 0.5	1 $\pm$ 0.2	47 $\pm$ 1	-19 $\pm$ 5.2	267 $\pm$ 100	103	1.32	0.84	2.69	1.49
	8.5 $\pm$ 0.2	1084 $\pm$ 5	13.32 $\pm$ 0.02	0.4 $\pm$ 0.2	69 $\pm$ 2	10 $\pm$ 1	127 $\pm$ 2	18 $\pm$ 2	101 $\pm$ 1	5 $\pm$ 0.5	1 $\pm$ 0.3	113 $\pm$ 2	-21 $\pm$ 6.9	288 $\pm$ 123	94	1.24	0.46	4.25	1.21
													-21 $\pm$ 6.9	288 $\pm$ 123	94	1.24	0.46	4.25	1.21
Natural water <sup>2</sup>	7.6 $\pm$ 0.2	777 $\pm$ 2	-	-	60 $\pm$ 2	75 $\pm$ 1	75 $\pm$ 2	15 $\pm$ 1	94 $\pm$ 2	2 $\pm$ 0.4	1 $\pm$ 0.1	46 $\pm$ 1	-18 $\pm$ 4.7	283 $\pm$ 119	97	2.02	2.90	5.46	3.57
	8.5 $\pm$ 0.2	1029 $\pm$ 3	13.05 $\pm$ 0.1	6.6 $\pm$ 1.3	69 $\pm$ 2	10 $\pm$ 1	127 $\pm$ 2	18 $\pm$ 2	101 $\pm$ 1	5 $\pm$ 0.3	1 $\pm$ 0.1	113 $\pm$ 2	-17 $\pm$ 7.1	299 $\pm$ 129	N.	1.52	0.80	3.62	1.31
													-17 $\pm$ 7.1	299 $\pm$ 129	N.	1.52	0.80	3.62	1.31
														Reference 1 <sup>3</sup>	98	2.01	0.31	4.07	0.32
														Reference 2	100	1.66	0.15	3.89	0.22
														Reference 3	104	1.38	0.11	3.25	0.20

<sup>1</sup>  $R_{hDLS}$  was measured before injection experiments.

<sup>2</sup> For filtered natural water and natural water, all the data are listed in two rows because experiment 3 was conducted 2 years later than experiment 1&2 and natural water quality for experiment 3 differed from the previous 1&2.

<sup>3</sup> Reference 1–3 are the simulations of NaCl injection experiments in Demi water.

\* N.D. Not determined, due to erroneous initial concentrations ( $C_0$ ).

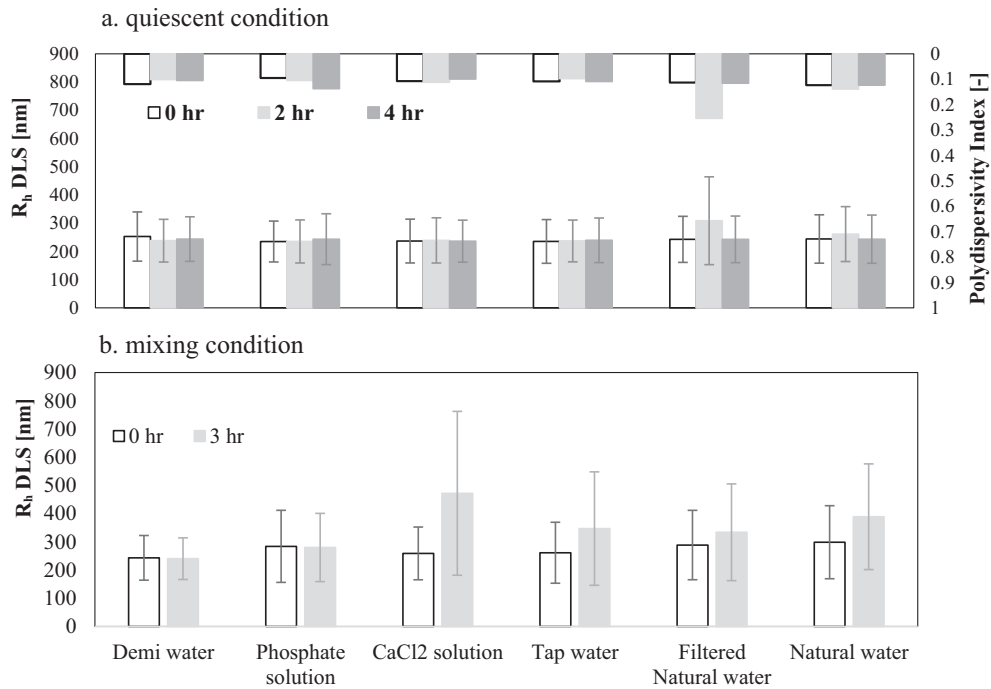


**Fig. 2.**  $R_{hDLS}$  of Si-DNA microparticles in 6 water types as a function of time (a. quiescent condition and b. mixing condition). The error bar represents the standard deviation of the size distribution. Polydispersity index (PDI) is equal to the square of standard deviation of the size distribution divided by the square of the mean.

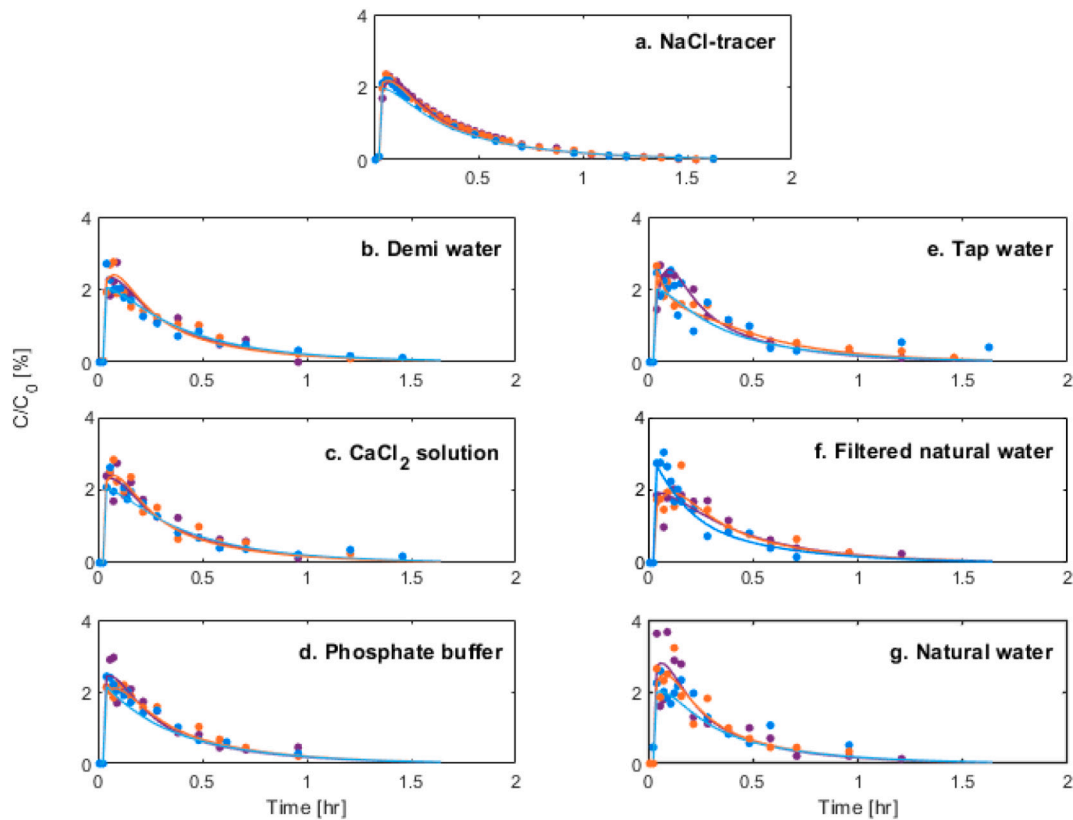


**Fig. 3.** Observed and simulated BTCs of Si-DNA microparticles in 6 water types plotted in relative concentration  $C/C_0$  [%]. The observed data are shown as solid circles in purple, orange, and blue for the 1st, 2nd, and 3rd replicate experiment, respectively. The corresponding simulated BTC is shown as line in purple, orange, and blue for 1st, 2nd, and 3rd replicate experiment, respectively. The observed and simulated BTCs of NaCl are shown for reference in plot a. (For interpretation of the references to colour in this figure legend, the reader is referred to the web version of this article.)

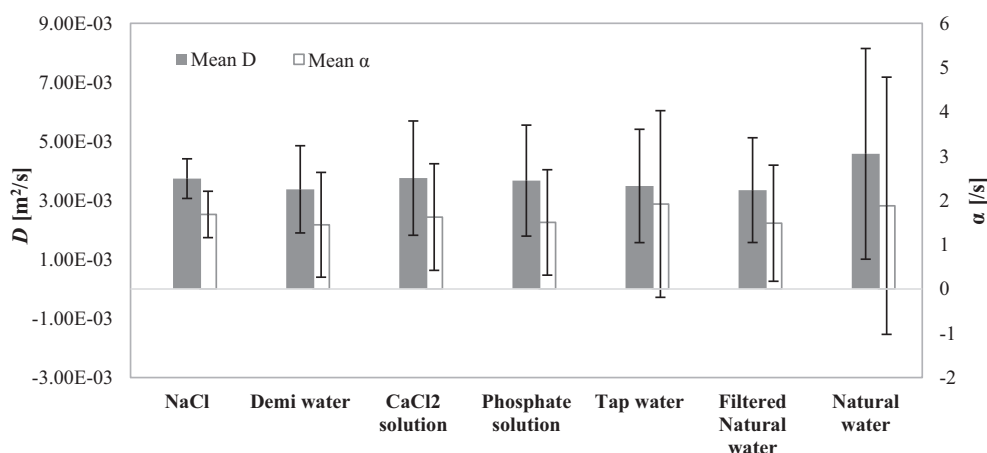


Fig. 4. Mean estimate of  $D_{Si-DNA}$  &  $\alpha_{Si-DNA}$  in comparison to  $D_{NaCl}$  &  $\alpha_{NaCl}$  with error bars showing approximate 95% confidence limits.

rest of BTCs of Si-DNA microparticles.

Regardless of solution chemistry and colloidal stability, mean  $D_{Si-DNA}$  was essentially similar across 6 water types and was comparable to  $D_{NaCl}$  (Fig. 4). The same was observed for the mean  $\alpha_{Si-DNA}$ . The size of the confidence intervals of  $D_{Si-DNA}$  and  $\alpha_{Si-DNA}$  were directly related to BTC noisy behavior. When we plotted the variations against relative concentration, we observed that uncertainties were more associated with tails than peaks of BTCs in all water types, of which natural waters (filtered and non-filtered) had the largest coefficient variations (Fig. S8). In natural waters, co-transporting with NOM and the likely presence of inorganic particles of various size ranges, Si-DNA microparticles were also subject to more complicated interactions such as steric, acid-base forces, etc. (Grasso et al., 2002), likely resulting in some random attachment and detachment (e.g., flocculation and breakage due to shear forces). This could possibly contribute to a more “irregular” or noisier Si-DNA BTC, resulting in a larger confidence interval/uncertainty of  $D_{Si-DNA}$  in natural waters.

Likewise, Schipperski et al. also showed a similar range of dispersion estimations of silica fluorescent particles of micron-size to those of solute tracers in a karst river drainage system, despite differences in the surface properties of the particle tracers (Schipperski et al., 2016). The effect of hydrodynamics on colloidal particle transport in subsurface environments is widely studied (Elimelech et al., 2013; Sasidharan et al., 2014; Torkzaban et al., 2007). However, in surface waters, less research focuses on quantitatively comparing colloids in the size range of 200–400 nm such as Si-DNA microparticles to that of solutes. Recently, DNA-tagged alginate-coated microparticles with a similar negative surface-charge in stream injection experiments showed to behave similarly to solute tracers in rising limb and peak of BTCs, albeit without quantification (Pang et al., 2020). Besides, among the few studies, most used particles of much larger size (such as natural organic/inorganic particulates, fluorescent latex particles, *E.coli*, and titanium-dioxide particles), and focused on distribution and fate without quantification of dispersion behavior (Drummond et al., 2014; Jamieson et al., 2005; Karwan and Saiers, 2009; Newbold et al., 2005; Phillips et al., 2019; Spencer et al., 2011; Wyer et al., 2010).

### 3.3. Mass recovery and data uncertainty

The mass recovery of each injection experiment is of fundamental importance for quantifying transport behavior of Si-DNA microparticles. We analyzed all samples and randomly performed lab duplicates. The mass recovery of Si-DNA microparticles with known initial concentration was calculated and ranged between 88% and 118% (Table 1). In Demi water, where minimal impurity or interfering ion was present, the mass recoveries of Si-DNA microparticles ranged between 91 and 97%.

In such case, the Si-DNA mass was considered fully recovered. A mass ambiguity of less than 10% is well within the expected mass ambiguity range  $\sim \pm 20\%$  which is due to the accuracy of qPCR reading and uncertainty of particle concentration (Foppen et al., 2013; Paunescu et al., 2015). qPCR technology is only accurate on a logarithmic-scale. From our experimental data, the difference of Cq values between replicates varied from  $\sim 0.07$  to  $\sim 0.2$ , which resulted in a concentration difference of  $\pm 5\%$  ( $= 2^{0.07}$ ) to  $\pm 14.8\%$  ( $= 2^{0.2}$ ). Such variation/error of Cq values was inevitable because errors may propagate from pipetting or intrinsic variances of enzymatic efficiency due to minor temperature differences in the qPCR apparatus (Foppen et al., 2013). Besides, a variety of factors including the water quality of samples could also influence the enzymatic activity (Gibson et al., 2012; Zipper et al., 2003). Moreover, subsampling is required when transferring a large environmental sample size into a much smaller sample size for qPCR analysis. When taking subsamples, the sample volume has to contain a sufficient number of particles such that variations are statistically insignificant (Crowe, 2012). In samples with diluted Si-DNA microparticles, up to a 20% difference in particle concentration between two samples can arise from a few particles difference, resulting in qPCR signal variations when subsamples and replicates were taken for qPCR assay (Kittilä et al., 2019). This is most likely to encounter for samples collected from large-scale environmental water bodies. However, in our laboratory experiments, such quantification uncertainty associated with particle concentration was trivial, as the qPCR amplification result as a function of the particle concentration (the 10-fold dilution curve in the SI) suggested that the particle quantification by amplifying DNA was consistent over a range of particle concentration down to  $10^{-8}$  mg/mL. Additionally, we speculate that the discrete nature of such heavier-than-fluid particles with a certain spread of size distribution might be the origin of the fluctuations in BTCs (Won et al., 2019). It would be very convenient if the size distribution was very limited such that every particle is essentially subject to the identical transport characteristics. Future research is warranted to assess the possible impact of particle size distribution on Si-DNA microparticle transport in surface waters.

The differences in fluctuations of Si-DNA BTCs may arise from particle characteristics (e.g., particle size distributions), environmental conditions (e.g., hydrodynamic forces) and qPCR analytical methods, contributing to the overall more “irregularities” in Si-DNA BTCs than NaCl BTCs. A similar trend of fluctuations in Si-DNA BTC was also reported, even more evidently, in recent studies on DNA-tagged microparticles and their tracing applicability in environmental and hydrological investigations (e.g., (Pang et al., 2020; C. Wang et al., 2019)). Nevertheless, increasing the injected tracer mass and up-concentrating from a larger sample volume into a smaller sample volume could be beneficial for obtaining better quality BTCs (Kittilä et al.,

2019).

#### 4. Conclusion

We concluded that the transport behavior of Si-DNA microparticles resembled that of NaCl in surface-water relevant conditions, evidenced by BTCs with a similar range of  $D$ . With special attention paid to mass balance, the Si-DNA microparticles as colloids had overall more erratic BTCs than solute tracers, whereby the scatter increased a function of water quality complexity. The overall larger confidence interval of  $D_{Si-DNA}$  we contributed to the discrete nature of colloidal particles with a certain particle size distribution and possible minor shear-induced aggregation. This research established a solid methodological foundation for field application of Si-DNA microparticles in surface water tracing. Despite the fluctuations of signals in BTCs, Si-DNA microparticles possess promising potential as surrogates for colloids of sub-micron size in surface water tracing experiments.

#### Author contributions

The manuscript was written through contributions of all authors. All authors have given approval to the final version of the manuscript.

#### Declaration of Competing Interest

The authors declare that they have no known competing financial interests or personal relationships that could have appeared to influence the work reported in this paper.

#### Acknowledgment

Financial support was provided by the Netherlands Organisation for Scientific Research (NWO) grant STW14515 WaterTagging and by China Scholarship Council (CSC). We thank ETH for kindly making the DNA tracer available. We also thank Dr. Sulalit Bandyopadhyay for his comments and helpful suggestions for this paper, lab staff from TUDelft and IHE Delft for the lab-work support, and two PhD students in the group, Bahareh Kianfar and Swagatam Chakraborty, for the discussion on this research.

#### Appendix A. Supplementary data

Supplementary data to this article can be found online at <https://doi.org/10.1016/j.jconhyd.2021.103880>.

#### References

- Alimi, O.S., Farner Budarz, J., Hernandez, L.M., Tufenkji, N., 2018. Microplastics and Nanoplastics in aquatic environments: aggregation, deposition, and enhanced contaminant transport. *Environ. Sci. Technol.* 52 (4), 1704–1724. <https://doi.org/10.1021/acs.est.7b05559>.
- Aquilanti, L., Clementi, F., Landolfo, S., Nanni, T., Palpacelli, S., Tazioli, A., 2013. A DNA tracer used in column tests for hydrogeology applications. *Environ. Earth Sci.* 70 (7), 3143–3154. <https://doi.org/10.1007/s12665-013-2379-y>.
- Aquilanti, L., Clementi, F., Nanni, T., Palpacelli, S., Tazioli, A., Vivalda, P.M., 2016. DNA and fluorescein tracer tests to study the recharge, groundwater flowpath and hydraulic contact of aquifers in the Umbria-Marche limestone ridge (central Apennines, Italy). *Environ. Earth Sci.* 75 (7) <https://doi.org/10.1007/s12665-016-5436-5>.
- Auffan, M., Rose, J., Bottero, J.-Y., Lowry, G.V., Jolivet, J.-P., Wiesner, M.R., 2009. Towards a definition of inorganic nanoparticles from an environmental, health and safety perspective. *Nat. Nanotechnol.* 4 (10), 634–641.
- Azimzada, A., Jreije, I., Hadioui, M., Shaw, P., Farner, J.M., Wilkinson, K.J., 2021. Quantification and characterization of Ti-, Ce-, and Ag-nanoparticles in global surface waters and precipitation. *Environ. Sci. Technol.* 55 (14), 9836–9844.
- Barthelme, G., Pratsinis, S.E., Buggisch, H., 2003. Particle size distributions and viscosity of suspensions undergoing shear-induced coagulation and fragmentation. *Chem. Eng. Sci.* 58 (13), 2893–2902.
- Bencala, K.E., Gooseff, M.N., Kimball, B.A., 2011. Rethinking Hyporheic Flow and Transient Storage To Advance Understanding of Stream - Catchment Connections. 47 (March), pp. 1–9. <https://doi.org/10.1029/2010WR010066>.

- Choi, J., Harvey, W., Conklin, H., 2000. Characterizing Multiple Timescales of Stream and Storage Zone Interaction that Affect Solute Fate and Transport in Streams. 36(6), pp. 1511–1518.
- Crowe, C.T. (Clayton T.), 2012. Multiphase Flows with Droplets and Particles. CRC Press.
- Dahlke, H.E., Williamson, A.G., Georgakakos, C., Leung, S., Sharma, A.N., Lyon, S.W., Walter, M.T., 2015. Using concurrent DNA tracer injections to infer glacial flow pathways. *Hydrol. Process.* 29 (25) <https://doi.org/10.1002/hyp.10679>.
- Dalas, E., Koutsoukos, P.G., 1990. Phosphate Adsorption at the Porous Glass/Water and SiO<sub>2</sub>/Water Interfaces.
- Derjaguin, B., Landau, L., 1993. Theory of the stability of strongly charged lyophobic sols and of the adhesion of strongly charged particles in solutions of electrolytes. *Prog. Surf. Sci.* 43 (1–4), 30–59.
- Drummond, J.D., Davies-Colley, R.J., Stott, R., Sukias, J.P., Nagels, J.W., Sharp, A., Packman, A.I., 2014. Retention and remobilization dynamics of fine particles and microorganisms in pastoral streams. *Water Res.* 66, 459–472. <https://doi.org/10.1016/j.watres.2014.08.025>.
- Elimelech, M., Gregory, J., Jia, X., 2013. Particle Deposition and Aggregation: Measurement, Modelling and Simulation. Butterworth-Heinemann.
- Foppen, J.W., Orup, C., Adell, R., Poulalion, V., Uhlenbrook, S., 2011. Using multiple artificial DNA tracers in hydrology. *Hydrol. Process.* 25 (19), 3101–3106.
- Foppen, J.W., Seopa, J., Bakobie, N., Bogaard, T., 2013. Development of a methodology for the application of synthetic DNA in stream tracer injection experiments. *Water Resour. Res.* 49 (9), 5369–5380. <https://doi.org/10.1002/wrcr.20438>.
- Frungieri, G., Babler, M.U., Vanni, M., 2020. Shear-induced heteroaggregation of oppositely charged colloidal particles. *Langmuir* 36 (36), 10739–10749. <https://doi.org/10.1021/acs.langmuir.0c01536>.
- Garnett, M.C., Ferruti, P., Ranucci, E., Suardi, M.A., Heyde, M., Sleat, R., 2009. Sterically stabilized self-assembling reversibly cross-linked polyelectrolyte complexes with nucleic acids for environmental and medical applications. *Biochem. Soc. Trans.* 37 (4), 713–716. <https://doi.org/10.1042/BST0370713>.
- Gibson, K.E., Schwab, K.J., Spencer, S.K., Borchardt, M.A., 2012. Measuring and mitigating inhibition during quantitative real time PCR analysis of viral nucleic acid extracts from large-volume environmental water samples. *Water Res.* 46 (13), 4281–4291. <https://doi.org/10.1016/j.watres.2012.04.030>.
- Goepfert, N., Goldscheider, N., 2019. Improved understanding of particle transport in karst groundwater using natural sediments as tracers. *Water Res.* 166 <https://doi.org/10.1016/j.watres.2019.115045>.
- Göppert, N., Goldscheider, N., 2008. Solute and colloid transport in karst conduits under low- and high-flow conditions. *Ground Water* 46 (1), 61–68. <https://doi.org/10.1111/j.1745-6584.2007.00373.x>.
- Grasso, D., Subramaniam, K., Butkus, M., Strevett, K., Bergendahl, J., 2002. A review of non-DLVO interactions in environmental colloidal systems. In: *Re/Views in Environmental Science & Bio/Technology*, Vol. 1.
- Gregory, J., 2005. *Particles in Water: Properties and Processes*. CRC Press.
- Guo, L., Macdonald, R.W., 2006. Source and transport of terrigenous organic matter in the upper Yukon River: evidence from isotope ( $\delta^{13}C$ ,  $\Delta^{14}C$ , and  $\delta^{15}N$ ) composition of dissolved, colloidal, and particulate phases. *Glob. Biogeochem. Cycles* 20 (2).
- Haggerty, R., Argerich, A., Marti, E., 2008. Development of a “smart” tracer for the assessment of microbiological activity and sediment-water interaction in natural waters: the resazurin-resorufin system. *Water Resour. Res.* 46 (4) <https://doi.org/10.1029/2007WR006670>.
- Harvey, J., Wagner, B., 2000. Quantifying hydrologic interactions between streams and their subsurface hyporheic structure. *Streams Ground Waters* 3–44. <http://ci.nii.ac.jp/naid/10025954970/en/>.
- Heathwaite, A.L., Dils, R.M., 2000. Characterising phosphorus loss in surface and subsurface hydrological pathways. *Sci. Total Environ.* 251, 523–538.
- Hijnen, N., Clegg, P.S., 2014. Colloidal aggregation in mixtures of partially miscible liquids by shear-induced capillary bridges. *Langmuir* 30 (20), 5763–5770.
- Jamieson, R., Joy, D.M., Lee, H., Kostaschuk, R., Gordon, R., 2005. Transport and deposition of sediment-associated *Escherichia coli* in natural streams. *Water Res.* 39 (12), 2665–2675. <https://doi.org/10.1016/j.watres.2005.04.040>.
- Jarvie, H.P., Neal, C., Rowland, A.P., Neal, M., Morris, P.N., Lead, J.R., Lawlor, A.J., Woods, C., Vincent, C., Guyatt, H., 2012. Role of riverine colloids in macronutrient and metal partitioning and transport, along an upland–lowland land-use continuum, under low-flow conditions. *Sci. Total Environ.* 434, 171–185.
- Ji, W., Tang, Q., Shen, Z., Fan, M., Li, F., 2020. The adsorption of phosphate on hydroxylated alpha-SiO<sub>2</sub> (001) surface and influence of typical anions: a theoretical study. *Appl. Surf. Sci.* 501 <https://doi.org/10.1016/j.apsusc.2019.144233>.
- Karwan, D.L., Sayers, J.E., 2009. Influences of seasonal flow regime on the fate and transport of fine particles and a dissolved solute in a New England stream. *Water Resour. Res.* 45 (11), 1–9. <https://doi.org/10.1029/2009WR008077>.
- Kittilä, A., Jalali, M.R., Evans, K.F., Willmann, M., Saar, M.O., Kong, X.Z., 2019. Field comparison of DNA-labeled nanoparticle and solute tracer transport in a fractured crystalline rock. *Water Resour. Res.* 55 (8), 6577–6595. <https://doi.org/10.1029/2019WR025021>.
- Lead, J.R., Wilkinson, K.J., 2006. Aquatic colloids and nanoparticles: current knowledge and future trends. *Environ. Chem.* 3 (3), 159–171.
- Lead, J.R., Batley, G.E., Alvarez, P.J.J., Handy, R.D., Mclaughlin, M.J., 2018. *Nanomaterials in the Environment: Behavior, Fate, Bioavailability, and Effects — An Updated Review*, 37, pp. 2029–2063. <https://doi.org/10.1002/etc.4147>, 8.
- Ledin, A., Karlsson, S., 1993. Effects of pH, Ionic Strength and a Fulvic Acid on Size Distribution and Surface Charge of Colloidal Quartz and Hematite, 8, pp. 2–7.
- Leibundgut, C., Seibert, J., 2011. *Tracer Hydrology. Treatise on Water Science*, January 2016, pp. 215–236. <https://doi.org/10.1016/B978-0-444-53199-5.00036-1>.

- Liao, R., Zhang, J., Li, T., Luo, D., Yang, D., 2020. Biopolymer/plasmid DNA microspheres as tracers for multiplexed hydrological investigation. *Chem. Eng. J.* 401 <https://doi.org/10.1016/j.cej.2020.126035>.
- Lindahl, T., 1993. Instability and Decay of the Primary Structure of DNA.
- Liu, X., Wazne, M., Chou, T., Xiao, R., Xu, S., 2010. Influence of Ca<sup>2+</sup> and Suwannee River humic acid on aggregation of silicon nanoparticles in aqueous media. *Water Res.* 45 (1), 105–112. <https://doi.org/10.1016/j.watres.2010.08.022>.
- Mahler, B.J., Matthew, W., Philip, B., Hillis, D.M., 1998. DNA-labeled clay: a sensitive new method for tracing particle transport. *Geology* 26 (9), 831–834. [https://doi.org/10.1130/0091-7613\(1998\)026<0831:DLCASN>2.3.CO;2](https://doi.org/10.1130/0091-7613(1998)026<0831:DLCASN>2.3.CO;2).
- McCarthy, J., Zachara, J., 1989. ES&T Features: subsurface transport of contaminants. *Environ. Sci. Technol.* 23 (5), 496–502.
- McCarthy, J.F., McKay, L.D., Bruner, D.D., 2002. Influence of ionic strength and cation charge on transport of colloidal particles in fractured shale saprolite. *Environ. Sci. Technol.* 36 (17), 3735–3743.
- McCluskey, J., Flores, M.E., Hinojosa, J., Jafarzadeh, A., Moghadam, S.v., Phan, D.C., Green, R.T., Kapoor, A.S., 2021. Tracking water with synthetic DNA tracers using droplet digital PCR. *ACS ES&T Water*. <https://doi.org/10.1021/acsestwater.0c00245>.
- Metin, C.O., Bonnacaze, R.T., Lake, L.W., Miranda, C.R., Nguyen, Q.P., 2014. Aggregation kinetics and shear rheology of aqueous silica suspensions. *Appl. Nanosci. (Switzerland)* 4 (2), 169–178. <https://doi.org/10.1007/s13204-012-0185-6>.
- Mikutis, G., Deuber, C.A., Schmid, L., Kittila, A., Lobsiger, N., Puddu, M., Asgeirsson, D.O., Grass, R.N., Saar, M.O., Stark, W.J., 2018. Silica-Encapsulated DNA-Based Tracers for Aquifer Characterization. <https://doi.org/10.1021/acs.est.8b03285>.
- Nantke, C.K.M., Frings, P.J., Stadmark, J., Czymzik, M., Conley, D.J., 2019. Si cycling in transition zones: a study of Si isotopes and biogenic silica accumulation in the Chesapeake Bay through the Holocene. *Biogeochemistry* 146 (2), 145–170. <https://doi.org/10.1007/s10533-019-00613-1>.
- Newbold, J.D., Thomas, S.A., Minshall, G.W., Cushing, C.E., Georgian, T., 2005. Deposition, benthic residence, and resuspension of fine organic particles in a mountain stream. *Limnol. Oceanogr.* 50 (5), 1571–1580. <https://doi.org/10.4319/lo.2005.50.5.1571>.
- Nocito-Gobel, J., Tobiason, J.E., 1996. Effects of ionic strength on colloid deposition and release. *Colloids Surf. A Physicochem. Eng. Asp.* 107, 223–231.
- Oney, D.M., Nason, J.A., 2021. Natural organic matter surface coverage as a predictor of heteroaggregation between nanoparticles and colloids. *Environ. Sci. Nano* 8 (3), 687–697.
- Pang, L., Farkas, K., Bennett, G., Varsani, A., Easingwood, R., Tilley, R., Nowostawska, U., Lin, S., 2014. Mimicking filtration and transport of rotavirus and adenovirus in sand media using DNA-labeled, protein-coated silica nanoparticles. *Water Res.* 62 <https://doi.org/10.1016/j.watres.2014.05.055>.
- Pang, L., Robson, B., Farkas, K., McGill, E., Varsani, A., Gillot, L., Li, J., Abraham, P., 2017. Tracking effluent discharges in undisturbed stony soil and alluvial gravel aquifer using synthetic DNA tracers. *Sci. Total Environ.* 592, 144–152. <https://doi.org/10.1016/j.scitotenv.2017.03.072>.
- Pang, L., Abeyskera, G., Hanning, K., Premaratne, A., Robson, B., Abraham, P., Sutton, R., Hanson, C., Hadfield, J., Heiligenthal, L., Stone, D., McBeth, K., Billington, C., 2020. Water tracking in surface water, groundwater and soils using free and alginate-chitosan encapsulated synthetic DNA tracers. *Water Res.* 184 <https://doi.org/10.1016/j.watres.2020.116192>.
- Paunescu, D., Puddu, M., Soellner, J.O.B., Stoessel, P.R., Grass, R.N., 2013. Reversible DNA encapsulation in silica to produce ROS-resistant and heat-resistant synthetic DNA “fossils”. *Nat. Protoc.* 8 (12), 2440–2448. <https://doi.org/10.1038/nprot.2013.154>.
- Paunescu, D., Mora, C.A., Querci, L., Heckel, R., Puddu, M., Hattendorf, B., Günther, D., Grass, R.N., 2015. Detecting and number counting of single engineered nanoparticles by digital particle polymerase chain reaction. *ACS Nano* 9 (10), 9564–9572. <https://doi.org/10.1021/acsnano.5b04429>.
- Peijnenburg, W.J.G.M., Baalousha, M., Chen, J., von Der, F., Kuhlbusch, T.A.J., Lead, J., Nickel, C., Quik, J.T.K., Renker, M., Wang, Z., Albert, A., von Der, F., Kuhlbusch, T.A.J., Lead, J., Nickel, C., Quik, J.T.K., Renker, M., Wang, Z., Koelmans, A.A., Review, A., 2015. Technology A Review of the Properties and Processes Determining the Fate of Engineered Nanomaterials in the Aquatic Environment Determining the Fate of Engineered, p. 3389. <https://doi.org/10.1080/10643389.2015.1010430>.
- Petosa, A.R., Jaisi, D.E.B.P., Quevedo, I.R., Elimelech, M., 2010. Aggregation and Deposition of Engineered Nanomaterials in Aquatic Environments: Role of Physicochemical Interactions, 44, pp. 6532–6549, 17.
- Phillips, C.B., Dallmann, J.D., Jerolmack, D.J., Packman, A.I., 2019. Fine-particle deposition, retention, and resuspension within a sand-bedded stream are determined by streambed morphodynamics. *Water Resour. Res.* 303–318. <https://doi.org/10.1029/2019wr025272>.
- Praetorius, A., Badetti, E., Brunelli, A., Clavier, A., Gallego-Urrea, J.A., Gondikas, A., Hasselöv, M., Hofmann, T., Mackevica, A., Marcomini, A., 2020. Strategies for determining heteroaggregation attachment efficiencies of engineered nanoparticles in aquatic environments. *Environ. Sci. Nano* 7 (2), 351–367.
- Ptak, T., Piepenbrink, M., Martac, E., 2004. Tracer tests for the investigation of heterogeneous porous media and stochastic modelling of flow and transport - a review of some recent developments. *J. Hydrol.* 294 (1–3), 122–163. <https://doi.org/10.1016/j.jhydrol.2004.01.020>.
- Puddu, M., Paunescu, D., Stark, W.J., Grass, R.N., 2014. Magnetically recoverable, thermostable, hydrophobic DNA/silica encapsulates and their application as invisible oil tags. *ACS Nano* 8 (3), 2677–2685. <https://doi.org/10.1021/nm4063853>.
- Quik, J.T.K., Velzeboer, I., Wouterse, M., Koelmans, A.A., 2013. Heteroaggregation and sedimentation rates for nanomaterials in natural waters. *Water Res.* 48, 269–279. <https://doi.org/10.1016/j.watres.2013.09.036>.
- Rieckermann, J., Neumann, M., Ort, C., Huisman, J.L., Gujer, W., 2005. Dispersion coefficients of sewers from tracer experiments. *Water Sci. Technol.* 52 (5), 123–133. <https://doi.org/10.2166/wst.2005.0124>.
- Runkel, R.L., 1998. One-Dimensional Transport with Inflow and Storage (OTIS): A Solute Transport Model for Streams and Rivers.
- Sabir, I.H., Torgersen, J., Haldorsen, S., Aleström, P., 1999. DNA tracers with information capacity and high detection sensitivity tested in groundwater studies. *Hydrogeol. J.* 7 (3), 264–272. <https://doi.org/10.1007/s100400050200>.
- Sabir, I.H., Haldorsen, S., Torgersen, J., Alestrom, P., Gaut, S., Colleuille, H., Pedersen, T., Kitterod, N., Alestrom, P., 2000. Synthetic DNA Tracers: Examples of their Application in Water Related Studies Center for Environmental Radioactivity (CERAD CoE) View Project Bone Development in Zebrafish View Project. <https://www.researchgate.net/publication/228794984>.
- Sasidharan, S., Torkzaban, S., Bradford, S.A., Dillon, P.J., Cook, P.G., 2014. Coupled effects of hydrodynamic and solution chemistry on long-term nanoparticle transport and deposition in saturated porous media. *Colloids Surf. A Physicochem. Eng. Asp.* 457, 169–179.
- Schiperski, F., Zirlwagen, J., Scheytt, T., 2016. Transport and attenuation of particles of different density and surface charge: a karst aquifer field study. *Environ. Sci. Technol.* 50 (15), 8028–8035. <https://doi.org/10.1021/acs.est.6b00335>.
- Sharma, A.N., Luo, D., Walter, M.T., 2012. Hydrological tracers using nanobiotechnology: proof of concept. *Environ. Sci. Technol.* 46 (16), 8928–8936. <https://doi.org/10.1021/es301561q>.
- Sharma, A., Foppen, J.W., Banerjee, A., Sawssen, S., Bachhar, N., Peddis, D., Bandyopadhyay, S., 2021. Magnetic nanoparticles to unique DNA tracers: effect of functionalization on Physico-chemical properties. *Nanoscale Res. Lett.* 16 (1) <https://doi.org/10.1186/s11671-021-03483-5>.
- Shevlin, D., O'Brien, N., Cummins, E., 2018. Silver engineered nanoparticles in freshwater systems – likely fate and behaviour through natural attenuation processes. In: *Science of the Total Environment*, Vol. 621. Elsevier B.V., pp. 1033–1046. <https://doi.org/10.1016/j.scitotenv.2017.10.123>.
- Spencer, K.L., Droppo, I.G., He, C., Grapentine, L., Exall, K., 2011. A novel tracer technique for the assessment of fine sediment dynamics in urban water management systems. *Water Res.* 45 (8), 2595–2606. <https://doi.org/10.1016/j.watres.2011.02.012>.
- Spicer, P.T., 1997. Shear-Induced Aggregation-Fragmentation: Mixing and Aggregate Morphology Effects. University of Cincinnati.
- Stern, D.A., Khanbilvardi, R., Alair, J.C., 2001. Description of Flow Through a Natural Wetland using Dye Tracer Tests, 18, pp. 173–184.
- Stolpe, B., Guo, L., Shiller, A.M., Hasselöv, M., 2010. Size and composition of colloidal organic matter and trace elements in the Mississippi River, Pearl River and the northern Gulf of Mexico, as characterized by flow field-flow fractionation. *Mar. Chem.* 118 (3–4), 119–128.
- Torkzaban, S., Bradford, S.A., Walker, S.L., 2007. Resolving the coupled effects of hydrodynamics and DLVO forces on colloid attachment in porous media. *Langmuir* 23 (19), 9652–9660.
- Torkzaban, S., Bradford, S.A., van Genuchten, M.T., Walker, S.L., 2008. Colloid transport in unsaturated porous media: the role of water content and ionic strength on particle straining. *J. Contam. Hydrol.* 96 (1–4), 113–127.
- Tsuji, S., Ushio, M., Sakurai, S., Minamoto, T., Yamanaka, H., 2017. Water temperature-dependent degradation of environmental DNA and its relation to bacterial abundance. *PLoS One* 12 (4). <https://doi.org/10.1371/journal.pone.0176608>.
- Velzeboer, I., Quik, J.T.K., van de Meent, D., Koelmans, A.A., 2014. Rapid settling of nanoparticles due to heteroaggregation with suspended sediment. *Environ. Toxicol. Chem.* 33 (8), 1766–1773. <https://doi.org/10.1002/etc.2611>.
- Verwey, E.J.W., 1947. Theory of the stability of lyophobic colloids. *J. Phys. Chem.* 51 (3), 631–636.
- Viccione, G., Cuomo, A., Guida, D., Foppen, J.W., 2014. Using artificial DNA as tracer in a bedrock river of the middle Bussento karst system. In: *Proceedings of the 7th International Conference on Engineering Mechanics, Structures, Engineering Geology, EMESEG14*, pp. 3–5.
- Wang, H., Adeleye, A.S., Huang, Y., Li, F., Keller, A.A., 2015. Heteroaggregation of Nanoparticles with Biocolloids and Geocolloids, 226, pp. 24–36. <https://doi.org/10.1016/j.cis.2015.07.002>.
- Wang, C., McNew, C.P., Lyon, S.W., Walter, M.T., Volkman, T.H.M., Abramson, N., Sengupta, A., Wang, Y., Meira Neto, A.A., Pangle, L., Troch, P.A., Kim, M., Harman, C., Dahlke, H.E., 2019. Particle tracer transport in a sloping soil lysimeter under periodic, steady state conditions. *J. Hydrol.* 569, 61–76. <https://doi.org/10.1016/j.jhydrol.2018.11.050>.
- Watson, J.D., Gilman, M., Witkowski, J., Genentech, I., 1992. Recombinant DNA Second Edition Mark Zoller.
- Whitmer, S., Baker, L., Wass, R., 2000. Loss of bromide in a wetland tracer experiment. *J. Environ. Qual.* 29 (6), 2043–2045. <https://doi.org/10.2134/jeq2000.00472425002900060043x>.
- Wilderer, P.A., 2011. Treatise on Water Science, Vol. 2.09.
- Won, J., Lee, D., Pham, K., Lee, H., Choi, H., 2019. Impact of particle size distribution of colloidal particles on contaminant transport in porous media. *Appl. Sci. (Switzerland)* 9 (5). <https://doi.org/10.3390/app9050932>.
- Wyer, M.D., Kay, D., Watkins, J., Davies, C., Kay, C., Thomas, R., Porter, J., Stapleton, C.M., Moore, H., 2010. Evaluating short-term changes in recreational water quality during a hydrograph event using a combination of microbial tracers, environmental microbiology, microbial source tracking and hydrological techniques: a case study in

- Southwest Wales, UK. *Water Res.* 44 (16), 4783–4795. <https://doi.org/10.1016/j.watres.2010.06.047>.
- Xu, L., Xu, M., Wang, R., Yin, Y., Lynch, I., Liu, S., 2020. The crucial role of environmental coronas in determining the biological effects of engineered Nanomaterials. In: *Small*. Wiley-VCH Verlag. <https://doi.org/10.1002/sml.202003691>. Vol. 16, issue 36.
- Zaccone, A., Wu, H., Gentili, D., Morbidelli, M., 2009. Theory of activated-rate processes under shear with application to shear-induced aggregation of colloids. *Phys. Rev. E Stat. Nonlinear Soft Matter Phys.* 80 (5) <https://doi.org/10.1103/PhysRevE.80.051404>.
- Zhao, J., Li, Y., Wang, X., Xia, X., Shang, E., Ali, J., 2021. Ionic-strength-dependent effect of suspended sediment on the aggregation, dissolution and settling of silver nanoparticles. *Environ. Pollut.* 279 <https://doi.org/10.1016/j.envpol.2021.116926>.
- Zhu, X., Munno, K., Grbic, J., Werbowski, L.M., Bikker, J., Ho, A., Guo, E., Sedlak, M., Sutton, R., Box, C., 2021. Holistic Assessment of Microplastics and Other Anthropogenic Microdebris in an Urban Bay Sheds Light on their Sources and Fate. *ACS ES&T Water*.
- Zipper, H., Buta, C., La, K., Brunner, H., Jurgen, B., Frank, V., 2003. Mechanisms Underlying the Impact of Humic Acids on DNA Quanti® Cation by SYBR Green I and Consequences for the Analysis of Soils and Aquatic Sediments. 31(7). <https://doi.org/10.1093/nar/gng039>.